LETTERS

Molecular identification of the CRAC channel by altered ion selectivity in a mutant of Orai

Andriy V. Yeromin[1]*, Shenyuan L. Zhang[1]*, Weihua Jiang[1], Ying Yu[1], Olga Safrina[1] & Michael D. Cahalan[1]

Recent RNA interference screens have identified several proteins that are essential for store-operated Ca^{2+} influx and Ca^{2+} release-activated Ca^{2+} (CRAC) channel activity in *Drosophila* and in mammals, including the transmembrane proteins Stim (stromal interaction molecule)[1,2] and Orai[3–5]. Stim probably functions as a sensor of luminal Ca^{2+} content and triggers activation of CRAC channels in the surface membrane after Ca^{2+} store depletion[1,6]. Among three human homologues of *Orai* (also known as *olf186-F*), *ORAI1* on chromosome 12 was found to be mutated in patients with severe combined immunodeficiency disease, and expression of wild-type Orai1 restored Ca^{2+} influx and CRAC channel activity in patient T cells[3]. The overexpression of Stim and Orai together markedly increases CRAC current[5,7–9]. However, it is not yet clear whether Stim or Orai actually forms the CRAC channel, or whether their expression simply limits CRAC channel activity mediated by a different channel-forming subunit. Here we show that interaction between wild-type Stim and Orai, assessed by co-immunoprecipitation, is greatly enhanced after treatment with thapsigargin to induce Ca^{2+} store depletion. By site-directed mutagenesis, we show that a point mutation from glutamate to aspartate at position 180 in the conserved S1–S2 loop of Orai transforms the ion selectivity properties of CRAC current from being Ca^{2+}-selective with inward rectification to being selective for monovalent cations and outwardly rectifying. A charge-neutralizing mutation at the same position (glutamate to alanine) acts as a dominant-negative non-conducting subunit. Other charge-neutralizing mutants in the same loop express large inwardly rectifying CRAC current, and two of these exhibit reduced sensitivity to the channel blocker Gd^{3+}. These results indicate that Orai itself forms the Ca^{2+}-selectivity filter of the CRAC channel.

Orai and Orai1 possess four hydrophobic stretches that are predicted to span the membrane. On the basis of strategies used previously for several different ion channels, we made point mutations to investigate the most conserved loop between putative transmembrane segments (Supplementary Fig. 1a) and examined properties of ion selectivity, current–voltage rectification and block that are intimately associated with a pore-forming subunit. Wild-type or mutant Orai proteins were overexpressed together with wild-type Stim in S2 cells; messenger RNA and protein expression were verified by RT–PCR and western blotting (Fig. 1a and Supplementary Fig. 1b). In addition, by co-immunoprecipitation of the epitope-tagged wild-type proteins, we evaluated whether Stim and Orai are associated with each other before and after Ca^{2+} store depletion. When cells were cultured without stimulation, only limited interaction was seen. However, Ca^{2+} store depletion triggered by thapsigargin, which inhibits the SERCA (sarco/endoplasmic reticulum Ca^{2+}-ATPase) re-uptake pump, markedly increased Stim–Orai protein interaction when either protein was used to pull down the other by co-immunoprecipitation (Fig. 1a). This result shows that both transfected proteins are expressed and, moreover, that they interact, either directly or as part of a complex, after Ca^{2+} store depletion to initiate CRAC channel activation. During whole-cell recording on the co-transfected cells, dialysis of a Ca^{2+} chelator (BAPTA) into the cytoplasm activated a very large Ca^{2+}-selective inward current, as shown previously[5]. Using a pipette solution that maintains normal Ca^{2+} store content to prevent spontaneous channel opening, we confirmed that addition of inositol-1,4,5-trisphosphate (IP_3) inside or thapsigargin (TG) outside resulted in greatly augmented CRAC current (Fig. 1b).

Expression of an Orai mutant with a glutamate-to-aspartate mutation at position 180 (Orai(E180D)), again together with wild-type Stim, generated a current that developed with the normal kinetics of CRAC current during passive Ca^{2+} store depletion, but also exhibited marked alterations in ion selectivity and rectification. In contrast to the normal inward CRAC current, Orai(E180D) expression produced a very large outward current and a smaller inward current that developed in parallel (Fig. 2a). Current–voltage (*I–V*) curves of the Orai(E180D)-induced current revealed an outwardly rectifying shape with a reversal potential of 6.0 ± 0.4 mV ($n = 14$ cells), in contrast to the characteristic inwardly rectifying

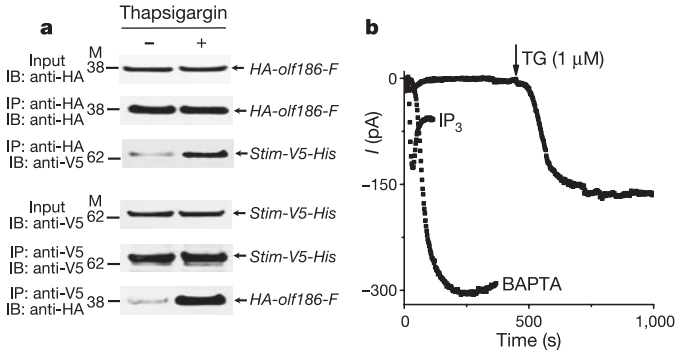

Figure 1 | Orai interacts with Stim and generates increased store-operated currents in S2 cells. a, Representative co-immunoprecipitation of Stim and Orai ($n = 3$). Input: total cell lysate, showing an equal amount of samples prepared for immunoprecipitation. Cells were transfected with *HA-olf186-F* (Orai) and *Stim-V5-His* (Stim) constructs, as indicated. M refers to molecular weight markers (kDa). **b**, Activation of CRAC current (at −130 mV) by three methods: IP_3 (10 μM IP_3 added to high-Ca^{2+} pipette solution; current density −11.4 ± 3.1 pA pF^{-1}, $n = 5$); thapsigargin (high-Ca^{2+} pipette solution and thapsigargin added to bath; −7.6 ± 2.5 pA pF^{-1}, $n = 2$); or passive store-depletion (Ca^{2+}-free pipette solution; −28.7 ± 1.8 pA pF^{-1}, $n = 27$). All three methods produced substantially greater CRAC current density than passive store depletion in control cells (−2.5 ± 0.4 pA pF^{-1}, $n = 18$).

[1]Department of Physiology & Biophysics and Center for Immunology, University of California, Irvine, California 92697, USA.
*These authors contributed equally to this work.

I–V curves with a reversal potential >50 mV of native or wild-type Orai-induced CRAC current (Fig. 2b).

In a series of ion-substitution experiments, we evaluated the ion selectivity properties of current induced by Orai(E180D). Substitution of Na^+ by choline while maintaining constant Ca^{2+} in the external solution—an experimental procedure that has little effect on native CRAC current[10] or CRAC current with overexpressed wild-type Orai (Fig. 2c)—reduced the inward current and shifted the reversal potential to hyperpolarized potentials (Fig. 2d), indicating that the Orai(E180D)-induced inward current is carried predominantly by Na^+ rather than by Ca^{2+}. Next, different divalent cation species in the external solution were tested, resulting in a *I–V* pattern of wild-type Orai-induced CRAC current similar to native CRAC current described previously[10]. Ca^{2+}, Sr^{2+} and Ba^{2+}(20 mM in each case, while maintaining high external Na^+) resulted in increased inward current (Fig. 2e), indicating that each of these divalent cations is permeant, whereas Mg^{2+} is relatively impermeant. In contrast, representative *I–V* curves of Orai(E180D)-induced current (shown in Fig. 2f with the same colour code for comparison with Fig. 2e) reveal an entirely different pattern. A tenfold increase of Ca^{2+} concentration ($[Ca^{2+}]$) in the external solution significantly decreased the outward current and did little to the small inward current. Substitution of 2 mM external Ca^{2+} by 20 mM Sr^{2+} had little effect; Mg^{2+} increased the current; and Ba^{2+} significantly increased the inward current while decreasing the outward current (Supplementary Fig. 2a). These results indicate that divalent cations block the outward current (carried by Cs^+) in the potency sequence $Ca^{2+} > Ba^{2+} > Sr^{2+} > Mg^{2+}$, and the inward current (carried by Na^+) in the potency sequence $Ca^{2+} \approx Sr^{2+} > Mg^{2+} > Ba^{2+}$. Together, these ion-substitution experiments indicate that the Orai(E180D) mutation transforms the CRAC channel from being selective for divalent cations to being a monovalent-selective channel that selects against, and indeed is blocked by, divalent cations.

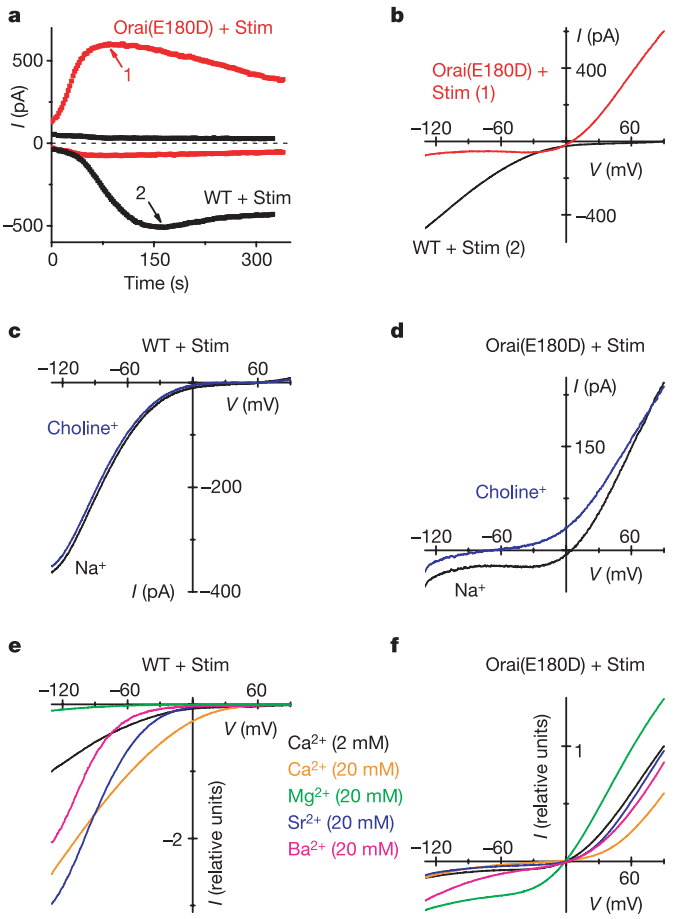

Figure 2 | Mutation E180D of Orai alters ion selectivity of the CRAC current. a, Time courses of inward current at −130 mV and outward current at 90 mV in representative cells overexpressing wild-type Orai (WT, black) or Orai(E180D) mutant (red). Ca^{2+}-free internal solution. **b**, *I–V* curves at times indicated in **a**. **c**, *I–V* curves of wild-type Orai-induced current in Ca2 solution containing 160 mM Na^+ and 2 mM Ca^{2+} and in choline external solution with 1.1 mM Na^+ and 2 mM Ca^{2+}. (Complete solution recipes are indicated in Supplementary Table 1.) **d**, Representative *I–V* curves for Orai(E180D) with the same solutions as **c** ($n = 3$). **e**, Divalent cation selectivity of wild-type Orai CRAC current. *I–V* curves are normalized to current values at −130 mV in Ca2 solution. Test solutions contained 20 mM test divalent and 124 mM Na^+. External solutions for **e** and **f** are labelled according to colour. **f**, *I–V* curves (not leak-subtracted) for Orai(E180D) with the same divalent cations, normalized to currents at 90 mV in Ca2 solution.

CRAC channels share with voltage-gated Ca^{2+} channels the property of monovalent ion permeation when external divalent ions are removed[11–15]. Upon withdrawal of external divalent cations, Na^+ carries significant current through CRAC channels, whereas Cs^+ is far less permeant[10,14,16,17]. The monovalent CRAC current normally declines within 10 s, a process termed depotentiation[15] that is due to removal of external Ca^{2+}. To check whether the Orai(E180D) mutation alters monovalent CRAC current, both wild-type- and Orai(E180D)-induced CRAC currents were recorded in divalent-free Na^+ and Cs^+ test solutions. Three clear differences can be discerned (Fig. 3). First, the inward Na^+ current was much larger in the Orai(E180D) mutant and did not depotentiate to the same extent as either wild-type Orai (Fig. 3a, b) or native CRAC current in S2 cells[10]. Second, in contrast to the relatively small Cs^+ current density in wild-type Orai (-1.6 ± 0.6 pA pF^{-1}, $n = 4$), Orai(E180D)-induced Cs^+ current density was much larger (-191 ± 46 pA pF^{-1}, $n = 4$), similar in amplitude to the Na^+ current (-238 ± 43 pA pF^{-1}, $n = 9$), and the large Cs^+ current did not depotentiate (Fig. 3b). Third, the measured reversal potential in Na^+ external solution was 7.9 ± 0.3 mV ($n = 9$) for Orai(E180D), whereas it was 52.4 ± 0.9 mV ($n = 5$) for wild-type Orai (Fig. 3c, d). Calculated from reversal potentials, the average permeability ratio P_{Na}/P_{Cs} changed from 8.0 for wild-type Orai to 1.4 as a result of the E180D mutation, indicating an increase in pore diameter or altered electrostatic interactions with cations. *I–V* curves for Orai(E180D)-induced current changed shape with varying external $[Ca^{2+}]$ (Fig. 3e), revealing voltage-dependent block (Fig. 3f) that causes outward rectification in physiological saline. This examination of ion selectivity properties shows that a conservative mutation of glutamate to aspartate at position 180 of Orai transforms the CRAC channel from being Ca^{2+}-selective and inwardly rectifying to one that conducts Na^+ or Cs^+ and is outwardly rectifying due to voltage-dependent Ca^{2+} block.

Expression of the charge-neutralizing Orai(E180A) mutant completely abolished native CRAC current (Fig. 4a), indicating that alanine-containing subunits prevent ion conduction in hetero-multimeric CRAC channels by a dominant-negative action. In contrast, expression of Orai(D184A), Orai(D186A) or Orai(N188A) mutants with Stim resulted in increased CRAC current with unaltered *I–V* shape (Fig. 4b) and normal monovalent Na^+ current that exhibited depotentiation and low Cs^+ permeability (data not shown). Figure 4c summarizes the effect of each Orai mutant tested on CRAC current density. Expressed by itself or together with Stim, only Orai(E180A) potently inhibited native CRAC current. The inward current density and *I–V* shape in cells expressing Orai(D184A), Orai(D186A) and Orai(N188A) mutants did not differ significantly from current observed in cells expressing wild-type Orai. Orai(E180D) was unique in producing very large outward currents as a result of altered ion selectivity.

Gd^{3+} very effectively suppresses native and wild-type Orai-induced CRAC current[5]. In addition to ion selectivity properties, block by Gd^{3+} was evaluated in all mutants (Fig. 4d). Two charge-neutralizing

mutations, aspartate to alanine at positions 184 and 186, and, to a lesser degree, mutation of asparagine to alanine at position 188, significantly reduced the potency of Gd^{3+} block (Fig. 4d and Supplementary Fig. 2b). As shown previously[5], wild-type Orai CRAC current was potentiated by 2-aminoethyldiphenyl borate (2-PB) at a low concentration (5 μM) and inhibited at a high (20 μM) concentration (Supplementary Fig. 3a), similar to effects of 2-APB on native CRAC current in Jurkat and in S2 cells[10,18]. The effects of 2-APB on Orai(E180D)-induced CRAC current were complex but still showed potentiation and inhibition (Supplementary Fig. 3b). The time course of Orai(E180D) outward CRAC current showed an immediate decrease preceding potentiation by 5 μM 2-APB, and an immediate increase preceding inhibition during 20 μM application ($n = 3$). The pharmacological analysis provides support for the conclusion that the S1–S2 loop is involved in ion selectivity and block by Gd^{3+}, and may contribute to the complex effects of 2-APB on CRAC current.

Our results demonstrate that thapsigargin-triggered store depletion dynamically strengthens an interaction between Stim and Orai, supporting a model for CRAC channel activation in which Stim serves as the Ca^{2+} sensor to detect store depletion and as the messenger to activate CRAC channels in the plasma membrane. More importantly, we conclude that Orai is a bona fide ion channel, based on the following: (1) RNA-interference-mediated knockdown of Orai expression suppresses thapsigargin-dependent Ca^{2+} influx and CRAC channel activity; (2) overexpression of Orai with or without Stim augments CRAC currents that exhibit biophysical properties identical to native CRAC current; and (3) mutations of negatively charged residues within the putative pore region of Orai significantly alter ion selectivity, current rectification and affinity to a charged channel blocker without altering channel activation kinetics. The marked alteration of these properties by a targeted point mutation provides definitive evidence that Orai embodies the pore-forming subunit of the CRAC channel.

The consensus sequence within the S1–S2 loop, 179VEVQLDxD186, contains the critical glutamate (bold) shown here to control ion selectivity properties of the CRAC channel, and two aspartates (underlined) that may help to attract Gd^{3+} (and Ca^{2+}) towards the pore. It is not similar to pore sequences found in other channels. Unlike the pore regions of voltage-gated Ca^{2+} (CaV) channels, which contain a relatively long loop and a ring of critical glutamates from different domains that form a high-affinity Ca^{2+}-binding site[19], the

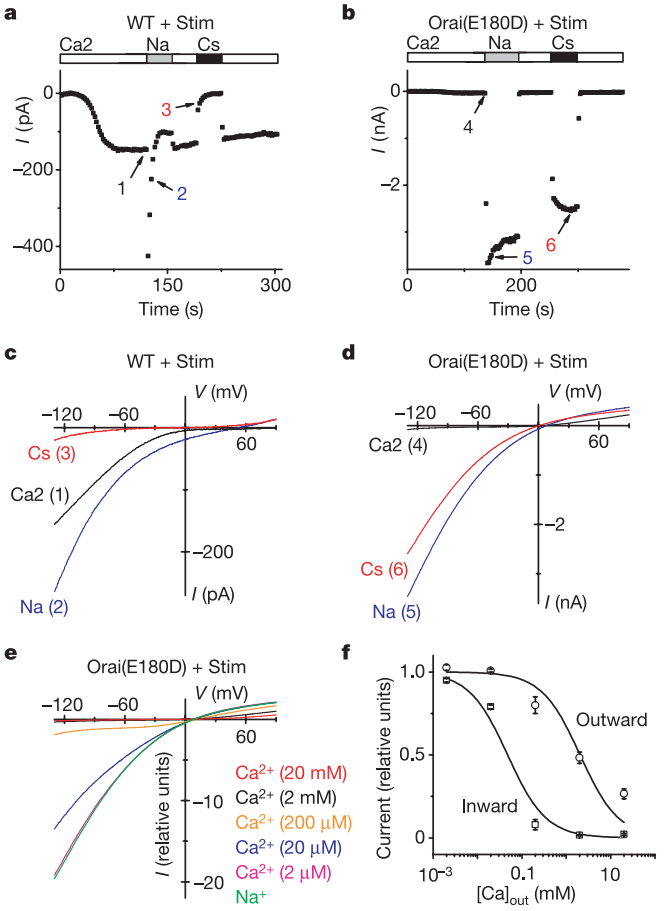

Figure 3 | Monovalent current in the absence of divalent ions exhibits altered ion selectivity in the Orai(E180D) mutant. **a**, Time course of inward current in a cell expressing wild-type Orai. Bars indicate external solution exchange. **b**, Same as **a** but for Orai(E180D). **c**, *I–V* curves for wild-type Orai at times indicated in **a**. **d**, *I–V* curves for Orai(E180D) at times indicated in **b**. **e**, *I–V* curves of Orai(E180D)-induced current in the presence of varying external $[Ca^{2+}]$. **f**, $[Ca^{2+}]$ dependence of Orai(E180D) CRAC current at −130 (squares) and 90 mV (circles), scaled to the current in divalent-free solution. Ca^{2+}-dependent block (mean ± s.e.m.) was fitted by the function $y = 1/(1 + [Ca^{2+}]/IC_{50})$, where IC_{50} is the calculated half-blocking Ca^{2+} concentration for inward current at −130 mV (48 ± 13 μM; $n = 13, 8, 4, 6$ and 2 cells for 20, 2, 0.2, 0.02 and 0.002 mM free external $[Ca^{2+}]$, respectively) and outward current at 90 mV (2.05 ± 0.78 mM; $n = 13, 8, 4, 5$ and 3 cells for 20, 2, 0.2, 0.02 and 0.002 mM free external $[Ca^{2+}]$, respectively).

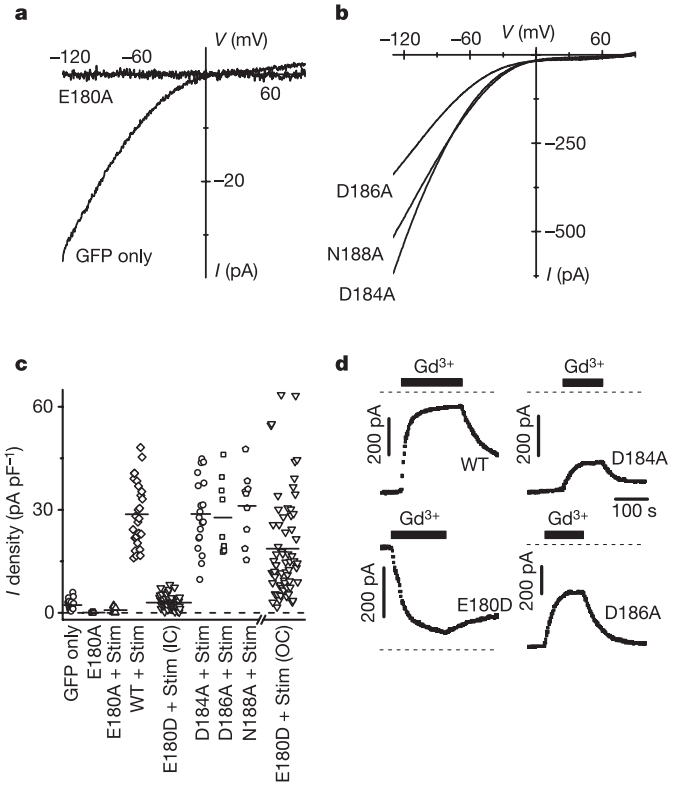

Figure 4 | Charge-neutralizing mutations in the S1–S2 loop. **a**, *I–V* curves in a cell expressing the Orai(E180A) mutant (without Stim) compared to control. **b**, *I–V* curves for Orai(D184A), Orai(D186A) and Orai(N188A) mutants. **c**, CRAC current density in transfected S2 cells. Each point represents the maximal CRAC current density (pA pF^{-1}) in a single cell, plotted as absolute values (from left to right): GFP-transfected control; Orai(E180A) ($P = 1.7 \times 10^{-4}$ relative to control); Orai(E180A) plus Stim ($P = 8.2 \times 10^{-3}$); wild-type Orai plus Stim; Orai(E180D) plus Stim, inward current; Orai(D184A) plus Stim; Orai(D186A) plus Stim; Orai(N188A) plus Stim; and Orai(E180D) plus Stim, outward current. **d**, Suppression of CRAC current by 5 nM Gd^{3+} in wild-type Orai and the D184A, E180D and D186A Orai mutants. Bars indicate time of Gd^{3+} application; dashed lines indicate the zero-current level.

putative pore sequence of Orai is very short, and the key residue for ion selectivity (E180) is adjacent to the putative S1 segment. Nevertheless, because withdrawal of external divalent ions reveals permeability to monovalent cations in both CaV[11,12] and CRAC channels[10,14,16,17], it is possible that the CRAC channel ion-selectivity filter is also formed by a ring of glutamates and that the mechanism of Ca^{2+} permeation is similar, although the single-channel conductance and maximum permeant ion size of the CRAC channel selectivity filter are smaller than that of the CaV channel[10,17,20,21]. Negatively charged side chains also contribute to Ca^{2+} selectivity of TRPV6; in this instance, aspartate (at position 541) is proposed to coordinate with Ca^{2+} ions and line the selectivity filter in a ring structure formed by four subunits[22]. The CRAC channel may be a multimer that includes several identical Orai subunits, as a non-conducting pore mutant (E180A) exerts a strong dominant-negative action on native CRAC current. Biochemical approaches and cysteine-scanning mutagenesis should be useful to elucidate better the unique pore architecture of the CRAC channel.

Note added in proof: While in proof, our attention was drawn to another paper reporting complementary findings regarding the control of ion selectivity in the CRAC channel[23]. In our study, the critical glutamate residue is 180 in the Orai protein encoded by the Invitrogen S2 cell complementary DNA (GenBank accession number DQ503470, as described[5]). The corresponding residue is 178 in the *Drosophila* genome database (accession number AY071273), and 106 in the human Orai1 homologue (accession number BC015369).

METHODS

Molecular cloning and mutagenesis. Generation of pAc5.1/EGFP, pAc5.1/D-STIM, pAc5.1/D-STIM-V5-His and pAc5.1/olf186-F (GenBank accession number DQ503470) were as described[5]. *Orai* pore mutants were made by exchanging the corresponding codons (E180A, GAG to GCG; E180D, GAG to GAC; D184A, GAT to GCT; D186A, GAT to GCT; N188A, AAT to GCT; Supplementary Fig. 1) using the QuikChange site-directed mutagenesis kit (Stratagene). The pAc5.1/HA-olf186-F clone was made by adding the haemagglutinin tag via PCR and re-cloned into the *Xho*I and *Not*I sites of pAc5.1/V5-His B expression vector. Resulting clones were confirmed by sequencing. Description of the primers and conditions for cloning are available upon request. Both HA-olf186-F and Stim-V5-His were verified for normal function by whole-cell recording.

Whole-cell recording. Cells transfected (Amaxa) with *Orai* and *Stim* constructs were identified by fluorescence of co-transfected GFP. Patch-clamp experiments were performed at room temperature in the standard whole-cell recording, using conditions similar to those reported previously[10]. The membrane capacitance of S2 cells selected for recording was 11.6 ± 0.4 pF ($n = 131$ cells). Membrane potentials were corrected for a liquid junction potential of 10 mV between the pipette and bath solution. The series resistance (2–7 MΩ) was not compensated. The membrane potential was held at −10 mV, and 220-ms voltage ramps from −130 to 90 mV alternating with 220-ms pulses to −130 mV were delivered every 2 s. Only cells with high input resistance (>2 GΩ) were selected for recording. External and pipette solution recipes are listed in Supplementary Table 1. Analysed data are presented as mean ± s.e.m.

Co-immunoprecipitation. Two days after transfection, 5×10^6 cells were treated with either Ringer's solution or zero-Ca^{2+} Ringer's solution plus 1 μM thapsigargin using solutions described[6] for 15 min at room temperature. Cells transfected with *Stim-V5-His* only or *HA-olf186-F* only were used as controls. Cell extracts were then prepared using RIPA lysis buffer (Upstate) according to the manufacturer's instructions. The extracts were pre-cleared with protein A/G beads (Pierce) and protein concentration was determined, using the Pierce BCA Protein Reagent Kit. The cell lysate was then diluted to approximately 1 mg ml^{-1} total protein with PBS and mixed with either anti-HA monoclonal antibodies (1 μg per 100 μg total protein, Santa Cruz) or anti-V5 monoclonal antibodies (1 μg per 100 μg total protein, Invitrogen) for 4 h at 4 °C. Equal amounts of samples were mixed with either normal mouse IgG or vehicle as negative controls. Protein A/G beads were subsequently added (1 μl per 1 μg IgG) to rock overnight at 4 °C. Proteins were eluted by boiling in 4× sample buffer (Invitrogen). Samples were resolved by SDS–PAGE and analysed by standard western blotting techniques. Anti-HA monoclonal antibodies (Santa Cruz) were used at a dilution of 1:200. Anti-V5 monoclonal antibodies (Invitrogen) were used at a dilution of 1:2,500. Proteins were detected by developing with the SuperSignal (Pierce) detection system. Samples treated with normal mouse IgG or vehicle showed no detectable signal for both *Stim-V5-His* and *HA-olf186-F* (data not shown), indicating that the immunoprecipitation and co-immunoprecipitation are specific.

Received 6 May; accepted 25 July 2006.
Published online 20 August 2006.

1. Liou, J. *et al.* STIM is a Ca^{2+} sensor essential for Ca^{2+}-store-depletion-triggered Ca^{2+} influx. *Curr. Biol.* **15,** 1235–1241 (2005).
2. Roos, J. *et al.* STIM1, an essential and conserved component of store-operated Ca^{2+} channel function. *J. Cell Biol.* **169,** 435–445 (2005).
3. Feske, S. *et al.* A mutation in Orai1 causes immune deficiency by abrogating CRAC channel function. *Nature* **441,** 179–185 (2006).
4. Vig, M. *et al.* CRACM1 is a plasma membrane protein essential for store-operated Ca^{2+} entry. *Science* **312,** 1220–1223 (2006).
5. Zhang, S. L. *et al.* Genome-wide RNAi screen of Ca^{2+} influx identifies genes that regulate Ca^{2+} release-activated Ca^{2+} channel activity. *Proc. Natl Acad. Sci. USA* **103,** 9357–9362 (2006).
6. Zhang, S. L. *et al.* STIM1 is a Ca^{2+} sensor that activates CRAC channels and migrates from the Ca^{2+} store to the plasma membrane. *Nature* **437,** 902–905 (2005).
7. Mercer, J. C. *et al.* Large store-operated calcium-selective currents due to co-expression of Orai1 or Orai2 with the intracellular calcium sensor, Stim1. *J. Biol. Chem.* doi:10.1074/jbc.M604589200 (published online 28 June 2006).
8. Peinelt, C. *et al.* Amplification of CRAC current by STIM1 and CRACM1 (Orai1). *Nature Cell Biol.* **8,** 771–773 (2006).
9. Soboloff, J. *et al.* Orai1 and STIM reconstitute store-operated calcium channel function. *J. Biol. Chem.* **281,** 20661–20665 (2006).
10. Yeromin, A. V., Roos, J., Stauderman, K. A. & Cahalan, M. D. A store-operated calcium channel in *Drosophila* S2 cells. *J. Gen. Physiol.* **123,** 167–182 (2004).
11. Almers, W. & McCleskey, E. W. Non-selective conductance in calcium channels of frog muscle: calcium selectivity in a single-file pore. *J. Physiol. (Lond.)* **353,** 585–608 (1984).
12. Hess, P. & Tsien, R. W. Mechanism of ion permeation through calcium channels. *Nature* **309,** 453–456 (1984).
13. Hoth, M. & Penner, R. Calcium release-activated calcium current in rat mast cells. *J. Physiol. (Lond.)* **465,** 359–386 (1993).
14. Lepple-Wienhues, A. & Cahalan, M. D. Conductance and permeation of monovalent cations through depletion-activated Ca^{2+} channels (ICRAC) in Jurkat T cells. *Biophys. J.* **71,** 787–794 (1996).
15. Zweifach, A. & Lewis, R. S. Calcium-dependent potentiation of store-operated calcium channels in T lymphocytes. *J. Gen. Physiol.* **107,** 597–610 (1996).
16. Kozak, J. A., Kerschbaum, H. H. & Cahalan, M. D. Distinct properties of CRAC and MIC channels in RBL cells. *J. Gen. Physiol.* **120,** 221–235 (2002).
17. Bakowski, D. & Parekh, A. B. Monovalent cation permeability and Ca^{2+} block of the store-operated Ca^{2+} current I_{CRAC} in rat basophilic leukemia cells. *Pflugers Arch.* **443,** 892–902 (2002).
18. Prakriya, M. & Lewis, R. S. Potentiation and inhibition of Ca^{2+} release-activated Ca^{2+} channels by 2-aminoethyldiphenyl borate (2-APB) occurs independently of IP_3 receptors. *J. Physiol. (Lond.)* **536,** 3–19 (2001).
19. Ellinor, P. T., Yang, J., Sather, W. A., Zhang, J. F. & Tsien, R. W. Ca^{2+} channel selectivity at a single locus for high-affinity Ca^{2+} interactions. *Neuron* **15,** 1121–1132 (1995).
20. Prakriya, M. & Lewis, R. S. Separation and characterization of currents through store-operated CRAC channels and Mg^{2+}-inhibited cation (MIC) channels. *J. Gen. Physiol.* **119,** 487–507 (2002).
21. Zweifach, A. & Lewis, R. S. Mitogen-regulated Ca^{2+} current of T lymphocytes is activated by depletion of intracellular Ca^{2+} stores. *Proc. Natl Acad. Sci. USA* **90,** 6295–6299 (1993).
22. Voets, T., Janssens, A., Droogmans, G. & Nilius, B. Outer pore architecture of a Ca^{2+}-selective TRP channel. *J. Biol. Chem.* **279,** 15223–15230 (2004).
23. Prakriya, M. *et al.* Orai1 is an essential pore subunit of the CRAC channel. *Nature* advance online publication, doi:10.1038/nature05122 (20 August 2006).

Supplementary Information is linked to the online version of the paper at www.nature.com/nature.

Acknowledgements We thank L. Forrest for assistance in cell culture and G. Chandy for use of molecular reagents in his laboratory. This work was supported by a grant from the National Institutes of Health (M.D.C.), by a fellowship from the George E. Hewitt Foundation (S.L.Z.), and by a Scientist Development Grant from the American Heart Association (Y.Y.).

Author Contributions A.V.Y. was responsible for all patch-clamp experiments and analysis. S.L.Z. was responsible for all molecular biology and biochemistry experiments, with the assistance of W.J. Y.Y. and O.S. performed RT-PCR. M.D.C. provided advice and overall direction, and supervised project planning and execution.

Author Information Reprints and permissions information is available at www.nature.com/reprints. The authors declare no competing financial interests. Correspondence and requests for materials should be addressed to M.D.C. (mcahalan@uci.edu).

SUPPLEMENTARY INFORMATION

Supplementary Methods

Cell culture and transfection

Drosophila S2 cells (Invitrogen) were propagated in Schneider's medium (Invitrogen) supplemented with 10% FBS at 24^{o}C. Cells were seeded at a density of 10^6 cells / ml and passaged when the cells achieved a density of ~6 x 10^6 cells / ml. S2 cells were transfected (see clones described in Methods) using a Nucleofector (Amaxa) following the manufacturer's protocol. Forty-eight hours post-transfection, cells were used for patch-clamp, biochemistry or processed for RT-PCR analysis.

Data analysis

Data were analyzed by Pulse (Heka Electronics) and Origin (OriginLab Corp.). Five *I-V* curves were averaged for display. Unless otherwise noted the displayed *I-V* curves are leak-subtracted. Since almost all S2 cells at the moment of break-in display an outward current that disappears during perfusion with internal solution (but before the inward CRAC current starts to develop), the following procedure for leak subtraction was employed. The first three ramp currents after the outward current subsided were averaged (I_{mid}). Then, another set of three ramps after maximal inward CRAC current had developed were averaged (I_{max}). The difference between I_{max} and I_{mid} represents an isolated CRAC current but with amplitude less than the actual one. To correct this the

difference was scaled such that the value of current at –130 mV is equal to maximal inward current minus initial inward current. Then the scaled difference was subtracted from I_{max} followed by fitting with a polynomial function. This fit was considered as the basal leak current. In a few cases (e.g. figure 4b) the initial outward current did not run down until the maximal inward current had developed. In this case a linear I-V curve reversing at 0 mV with current magnitude at +90 mV equal to the sustained outward current was assigned as leak current. For E180D *Orai*-induced CRAC current, the initial current was considered as leak.

RNA isolation and RT-PCR

RNA was isolated using TRIZOL (Invitrogen) following the manufacturer's protocols. The methods for RT-PCR were the same as described[6].

Supplementary Table 1. Solutions for whole-cell recording

Name	Na^+	Divalent / concentration	Ca^{2+} chelator / concentration	Cl^-	Sucrose
External (**Ca2**)	160	Ca^{2+} / 2	–	164	–
Choline external (**Chol**)	1.1	Ca^{2+} / 2	–	164	10
High-Ca^{2+} external (**Ca20**)	124	Ca^{2+} / 20	–	164	10
High-Mg^{2+} external (**Mg20**)	124	Mg^{2+} / 20	–	164	10
High-Sr^{2+} external (**Sr20**)	124	Sr^{2+} / 20	–	164	10
High-Ba^{2+} external (**Ba20**)	124	Ba^{2+} / 20	–	164	10
200 μM Ca^{2+} (**Ca 200μM**)	160	Ca^{2+} / 0.2	–	160	–
20 μM Ca^{2+} (**Ca 20μM**)	160	Ca^{2+} / 0.825	HEDTA / 2	162	–
2 μM Ca^{2+} (**Ca 2μM**)	160	Ca^{2+} / 0.85	EGTA / 2	162	–
Divalent-free Na^+ (**Na**)	152	–	HEDTA / 10	152	–
Divalent-free Cs^+ (**Cs**)	–	–	HEDTA / 10	160	–

Name	Cs^+ aspartate	Cs^+ BAPTA	CsCl	HEPES
Ca^{2+} - free internal	133	12	2	15
High-Ca^{2+} internal	152	–	–	10

Solution names used in figures are indicated in bold. Concentrations of ions and chemicals in the table are indicated in mM. External solutions contained 10 mM D-

glucose and 10 mM HEPES. Choline solution contained 160 mM of choline as choline chloride. Divalent-free Cs^+ solution contained 160 mM of Cs^+ as CsCl. Ca^{2+} - free internal solution contained 8 mM Mg gluconate. High-Ca^{2+} internal solution contained 1 mM $CaCl_2$, 6 mM $Ca(OH)_2$ and 10 mM EGTA. pH of external and internal solutions was 6.6 and 7.2 respectively and was adjusted by appropriate hydroxide. pH of choline solution was adjusted by NaOH. Osmolality was adjusted to 324 mOsm ± 1% by sucrose. Low Ca^{2+} solutions (Ca 20μM and Ca 2μM) were composed using estimates of free Ca^{2+} concentration provided by MaxChelator v. 2.50 (http://maxchelator.stanford.edu/) using tables cmc0204e.tmc and the following parameter settings: t = 23^0C, pH = 6.6, I = 179 (for Ca 20 μM) or I = 184 (for Ca 2 μM). Free Ca^{2+} concentration of high-Ca^{2+} internal solution estimated by MaxChelator was 450 nM. Gd^{3+} was added as $GdCl_3$. 2-APB was diluted from DMSO stock solution. IP_3 stock solution was prepared in water.

Supplementary Figure Legends

Supplementary Figure 1 Orai sequence, mutants, and expression. a, Partial protein sequence comparison shows an overall 67% identity (*) and 89% similarity (* and :) within the S1 - S2 region of *Drosophila Orai* and its human homologs. Putative transmembrane regions and mutation sites are indicated. **b**, Validation of effective mRNA overexpression. RT-PCR analysis was performed as described in Supplementary Methods using gene-specific primers. Overexpression of *Stim* with WT *Orai*, E180A, E180D, or D184A (left) and with WT *Orai*, D186A or N188A (right).

Supplementary Figure 2 Block of inward and outward CRAC current by divalent cations and gadolinium. a, Effect of divalent cations (20 mM) on E180D *Orai*-induced inward current (at –130 mV) and outward current (at 90 mV), normalized to currents in 2 mM Ca^{2+}. Mean ± SEM values are reported; the number of cells for each test divalent cation is indicated above the bars. Ca^{2+} ($P < 5x10^{-6}$ for outward current relative to 2 mM Ca^{2+} control); Ba^{2+} ($P = 6x10^{-4}$ for outward current and $7x10^{-5}$ for inward current); Sr^{2+} (NS); Mg^{2+} ($P = 0.01$ for outward current and 0.03 for inward current). The change in *I-V* shape with 20 mM external Ba^{2+} and increased inward current may result from incomplete block of inward Na^{+} current at negative potentials. **b**, Suppression of CRAC current by 5 nM Gd^{3+} in WT *Orai*; E180D; D184A ($P < 5x10^{-6}$ compared to WT); D186A ($P = 8x10^{-5}$); and N188A ($P = 1.5x10^{-3}$).

Supplementary Figure 3 Effect of 2-APB on CRAC current. a, WT *Orai*-induced CRAC current. Bars indicate time of 2-APB application at indicated concentrations. **b**, Same as **a** for the outward E180D *Orai*-induced CRAC current. Similar results were obtained in three separate experiments.

Cahalan 2006-06 Supplementary Figure 1

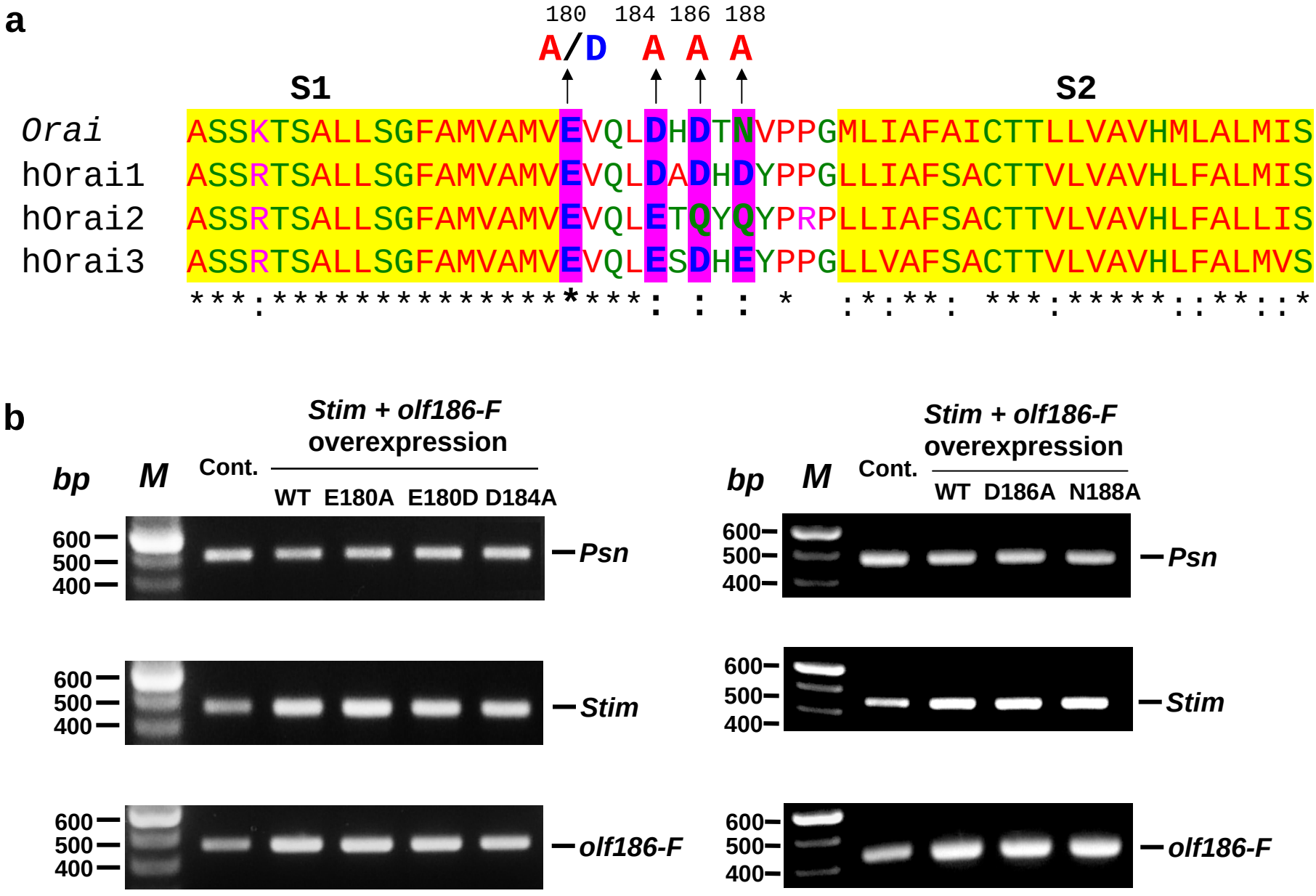

Cahalan 2006-06 Supplementary Figure 2

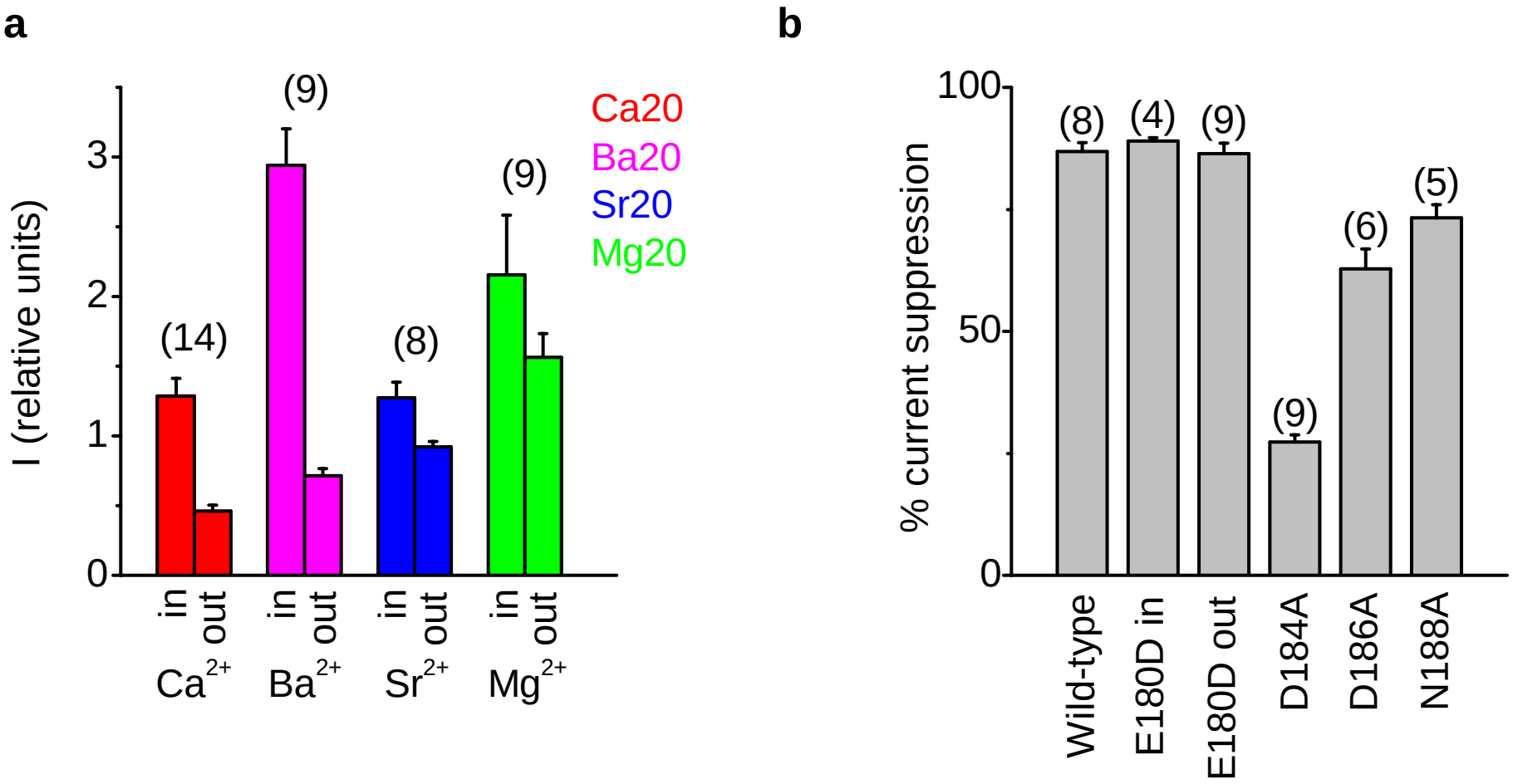

Cahalan 2006-06 Supplementary Figure 3